

A study on Matrix Element corrections in inclusive Z/γ^* production at LHC as implemented in PYTHIA, HERWIG, AlpGen and SHERPA.

P. Lenzi¹

Dept. of Physics, Università degli Studi di Firenze

J. M. Butterworth

Dept. of Physics and Astronomy, University College London

Abstract

We study Matrix Element corrections as implemented in four popular event generators for hadron collisions. We compare PYTHIA, HERWIG, AlpGen and SHERPA in the Z/γ^* inclusive production at LHC. PYTHIA and HERWIG are able to correct the first emission from the shower taking the Matrix Element calculation for one additional parton into account. SHERPA and AlpGen are able to take into account Matrix Element corrections not only for one, but rather for several hard emissions from the incoming partons. This can be done at the price of introducing a separation cut to distinguish a Matrix Element and a Parton Shower populated regions. In this paper we check the effect of Matrix Element corrections in PYTHIA and HERWIG and we check that results from these two generators are consistent. Then we turn to SHERPA and AlpGen, that implement two different methods to match Matrix Element calculations and Parton Shower. If we constraint them so that no more than one parton can emerge from the Matrix Element calculations they should both give results similar to PYTHIA and HERWIG. In other words PYTHIA and HERWIG provide us with the correct reference to spot possible issues with the matching prescriptions implemented in SHERPA and AlpGen. We also check to what extent the dependency on the Matrix Element - Parton Shower separation cut is canceled in these two generators.

¹piergiulio.lenzi@cern.ch

1 Introduction

The description of the QCD radiation pattern that accompanies the partons involved in a hard scattering process can be done at different precision levels. Most event generators attach the QCD radiation to the partons using the Parton Shower technique. While this approach provides a good description of many low p_T observables it may fail in efficiently filling the phase space for hard radiation. This limitation is connected to the Parton Shower being a collinear approximation of the description of parton splittings.

A way to improve the description of the QCD radiation pattern is to augment the Parton Shower with information coming from the exact matrix element calculation. The generators studied in this work follow this approach, but with significant differences. **PYTHIA** [1] and **HERWIG** [2, 3] are able to modify the shower in such a way that the hardest emission is described using the exact Matrix Element calculation for one additional real emission. **AlpGen** [4] and **SHERPA** [5] are able to take Matrix Element corrections for several (not only one) hard emissions. The main idea in both generators is that configurations in which the emitted partons' p_T is below a certain threshold are described with a pure Parton Shower approach, while configurations in which n partons are above the threshold are described with the n -real emissions Matrix Element. So, at the price of introducing an arbitrary threshold that is not present in **PYTHIA** or **HERWIG**, **AlpGen** and **SHERPA** should be able to describe the emission of several hard partons with the corresponding Matrix Element calculation. The dependency on the arbitrary threshold has to be as limited as possible.

In this paper we compare these different approaches for the case of the inclusive Z/γ^* production at LHC. We first check the effect of Matrix Element corrections in **PYTHIA** and **HERWIG**. We discuss the differences in the implementation and compare results from these two generators. Then, we discuss the differences in the merging prescriptions implemented in **SHERPA** and **AlpGen** and we present a sort of a consistency test about these prescriptions. The main idea behind this test is that if we allow the Matrix Element generators in **SHERPA** and **AlpGen** to emit not more than one additional parton we should recover results from **HERWIG** and **PYTHIA**, because we are using the same Matrix Element content. We also check to what extent the dependency on the threshold value in **AlpGen** and **SHERPA** is canceled.

2 Improving the description of the QCD radiation pattern using Matrix Element Calculations

In this section we briefly describe the implementation of the Matrix Element corrections in the generators studied in this work. We group the **PYTHIA** and **HERWIG**

implementations under the name of “Parton Shower reweighting”, while **SHERPA** and **AlpGen** belong to the category of “Matrix Element - Parton Shower merging”.

2.1 Parton Shower reweighting

In this section we describe the implementation of Matrix Element corrections in the Initial State Parton Shower as implemented in **PYTHIA**. We will enlight the differences between **HERWIG** and **PYTHIA** at the end of this section.

Matrix element corrections for inclusive Z/γ^* production in **PYTHIA** modifies the first emission from the PS so that the effect of the first order correction is reproduced. The lowest order graph contributing to Z/γ^* production is shown in Fig. 1. The processes that contribute to the first order correction are $q\bar{q} \rightarrow Z/\gamma^*g$, represented by the graphs in Fig. 2, and $qg \rightarrow Z/\gamma^*q$, represented by the graphs in Fig. 3.

The correction comes as a re-weighting factor of the parton shower. The initial state parton shower is weighted with two factors, one to reproduce the matrix elements of Fig. 2, $W_{q\bar{q} \rightarrow Z/\gamma^*g}$, and one to reproduce the matrix element of Fig. 3, $W_{qg \rightarrow Z/\gamma^*q}$ [6]. The PS emission closest to the hard $q\bar{q}$ process is the one that gets

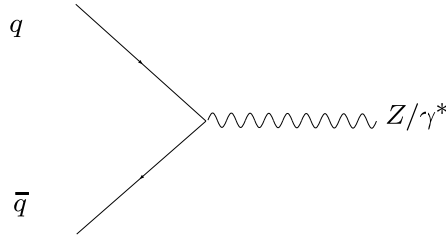


Figure 1: Lowest order contribution to the Z/γ^* production.

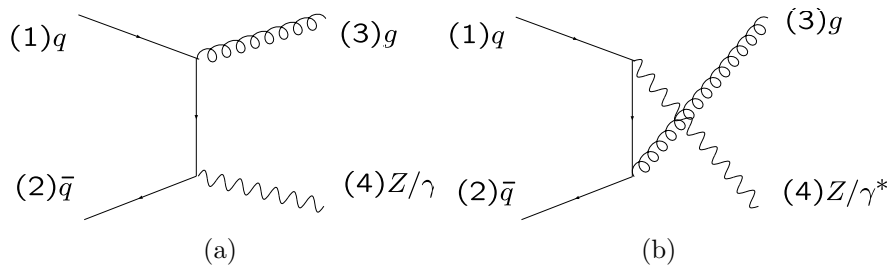


Figure 2: Graphs contributing to the $q\bar{q} \rightarrow Z/\gamma^*g$ process.

the correction. In order to correct the PS we need to classify this emission as either $(q\bar{q} \rightarrow Z/\gamma^*g)$ -like or $(qg \rightarrow Z/\gamma^*q)$ -like. A PS branching like the one depicted in Fig. 4 is considered $(q\bar{q} \rightarrow Z/\gamma^*g)$ -like, while a branching like the one in Fig. 5 is considered $(qg \rightarrow Z/\gamma^*q)$ -like.

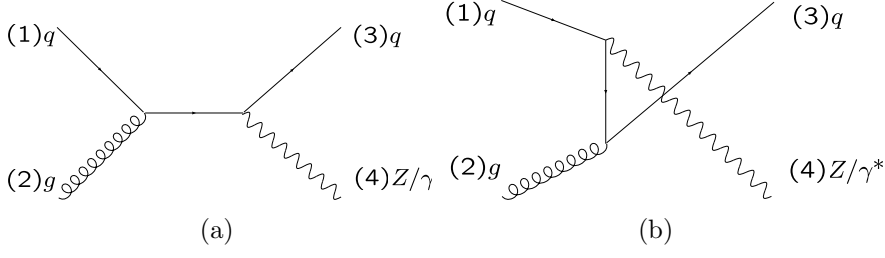


Figure 3: Graphs contributing to the $qg \rightarrow Z/\gamma^* q$.

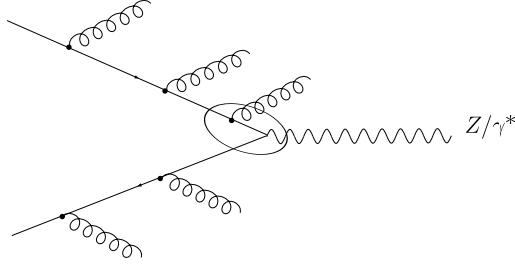


Figure 4: The circled PS branching is considered of type $q\bar{q} \rightarrow Z/\gamma^* g$.

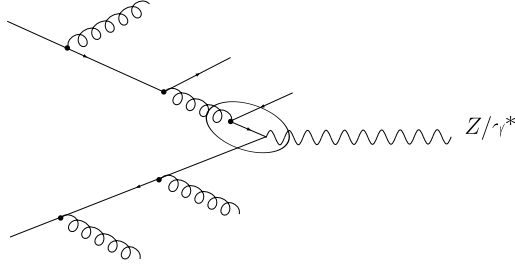


Figure 5: The circled PS branching is considered of type $qg \rightarrow Z/\gamma^* q$.

The ratio of the ME and PS differential cross sections, classified as described above, leads to the following expressions for $W_{q\bar{q} \rightarrow Z/\gamma^* g}$ and $W_{qg \rightarrow Z/\gamma^* q}$ [6]:

$$W_{q\bar{q} \rightarrow Z/\gamma^* g} = \frac{\hat{t}^2 + \hat{u}^2 + 2m_Z^2 \hat{s}}{\hat{s}^2 + m_Z^4}, \quad (1)$$

$$W_{qg \rightarrow Z/\gamma^* q} = \frac{\hat{s}^2 + \hat{u}^2 + 2m_Z^2 \hat{t}}{(\hat{s} - m_Z^2)^2 + m_Z^4}, \quad (2)$$

where \hat{s} , \hat{t} and \hat{u} are the Mandelstam variables. It can be shown that

$$\frac{1}{2} < W_{q\bar{q} \rightarrow Z/\gamma^* g} < 1, \quad (3)$$

and

$$1 < W_{qg \rightarrow Z/\gamma^* q} < 3. \quad (4)$$

This means that the Parton Shower alone would overestimate the $q\bar{q} \rightarrow Z/\gamma^*g$ contribution and underestimate the $qg \rightarrow Z/\gamma^*q$ contribution.

As described in [6] the correction is performed in two steps: first the starting scale for the shower is raised to the hadronic center of mass energy, so that any hard emission from the shower is kinematically possible; then the first splitting from the shower is classified as $(q\bar{q} \rightarrow Z/\gamma^*g)$ -like or $(qg \rightarrow Z/\gamma^*q)$ -like and the splitting probability is modified according to the corresponding W function.

Matrix element corrections are implemented in **HERWIG** in a similar way, but with two important differences:

- in **HERWIG** the PS is angular ordered, which means that the early emissions are soft large angle gluons; thus, the emission that deserves the corrections is not the first like in **PYTHIA**, as pointed in [7];
- in **HERWIG** the PS cannot fill the phase space for values above the hard scale of the process; in this respect it is similar to **PYTHIA** with starting scale set to M_Z .

For these reasons a two-step approach is used in **HERWIG** to implement ME corrections [8]. In the phase space region covered by the PS, corrections are applied as in **PYTHIA**, the only difference being that not the first emission, but rather the *hardest emission so far* during the shower evolution gets the correction [7]. These corrections are referred to as “soft ME corrections”. In the “dead zones”, that are left completely uncovered by the PS, the exact ME for one additional parton is used, with subsequent PS. These corrections are referred to as “hard ME corrections”.

2.2 Matrix Element - Parton Shower merging

SHERPA and **AlpGen** implement matrix element corrections in a different ways. They both subdivide the phase space in two regions, one for jet production which is filled by the Matrix Element calculation, and one for the jet evolution, which is filled by the Parton Shower. The criterion that is used to distinguish the two regions is a jet measure based cut.

The procedure implemented in **SHERPA** is known as CKKW merging. It was first proposed for lepton collisions in [9], then it was extended to hadron collisions in [10]. In a nutshell, the prescription foresees a preliminary step in which cross sections are calculated for up to n additional partons in the final state; ME level events are produced according to the calculated cross sections and they are weighted with a Sudakov weight that makes these states exclusive. In other words the Sudakov weight accounts for the probability that, given an n parton final state, no further hard emission is done by the Parton Shower; the reason for this is that any additional hard emission is going to be simulated by the $n + 1$ Matrix Element.

More extensively, the whole procedure foresees the following steps:

1. ME cross sections $\sigma_{n,i}$ are calculated for each parton multiplicity n and for each different combination i of partons that contributes to multiplicity n . A cutoff y_{cut} on the separation of partons is applied to avoid divergences. A fixed α_S^{ME} is used.
2. One among configurations n, i is selected with probability $P_{n,i} = \sigma_{n,i} / \sum_{m,j} \sigma_{m,j}$.
3. Parton momenta are generated according to the corresponding matrix element squared.
4. The scales at which the splittings happened are reconstructed: this is achieved through a k_\perp clustering of the partons emerging from the ME. The clustering is stopped when the core $2 \rightarrow 2$ process is found. This leads to a series of $n - 2$ clusterings with associated values of the k_\perp distance $y_2 \dots y_n$. Once the values $y_i = t_i^2/s$ are known we can finally calculate the ME event weight, that comes in two factors:
 - an α_S correction: for each clustering i an α_S correction $\alpha_S(t_i)/\alpha_S^{ME}$ is applied;
 - a Sudakov form factor correction is applied, to make states exclusive.
5. Events are accepted or rejected according to their weight.
6. The accepted events are showered with a veto on the emission above y_{cut} .

The matching prescription implemented in **AlpGen** is known as MLM [11]. It is similar in the motivations to the CKKW, but different in the implementation. Basically, instead of calculating Sudakov weights analytically, the event weighting is performed numerically. As in CKKW, ME cross sections are calculated up to the maximum parton multiplicity that the user wants in the final state; a minimum p_T cut for final state partons is used to cutoff ME divergences and a fixed α_S is used. As in CKKW a “PS history” is reconstructed and a splitting sequence is identified, with corresponding scales; an α_S correction is applied as in the CKKW. From this point the two prescriptions become different. In the MLM approach a conventional PS program is used (**PYTHIA** or **HERWIG**) and ME partons are showered without any constraint. The parton collection that results from the PS step is clustered using a jet algorithm (a cone in the **AlpGen** implementation, but also other options have been investigated, e.g. a k_\perp algorithm is used in **MADGRAPH/MADEVENT**); the resulting jets are matched in angle to the ME partons and only those events in which all the jets match the ME partons without any extra unmatched jets are retained (for the maximum ME parton multiplicity additional jets, softer than the matched ones, are allowed).

This procedure tries to reproduce in one go the effect that in the CKKW is achieved in two steps: the Sudakov re-weighting and the vetoed shower. Indeed the rejection of events with additional jets should, at the same time, reject ME

configuration in a similar way as the Sudakov weight does and prevent additional emission from the shower, thus reproducing the effect of the CKKW PS veto.

The MLM prescription is really convenient because it does not require modifications in the PS program. It just requires a veto routine to kill events not fulfilling the matching criteria.

While the CKKW prescription contains one parameter (the q_{cut} of the internal k_{\perp} clustering algorithm), in the MLM the user has to choose different parameters. The cone algorithm used for the matching has three parameters, namely the minimum jet p_T the cone radius R , and the jet maximum pseudorapidity η . The minimum p_T used in the cone clustering ($p_{T_{min}}^{jet}$) is not the same as the minimum p_T used in the ME step to cutoff divergences ($p_{T_{min}}^{ME}$): usually it is recommended to have $p_{T_{min}}^{jet} > p_{T_{min}}^{ME}$; this is needed because events that are below the cut at the ME level could fall above after the PS. For this reason a process dependent tuning for $p_{T_{min}}^{jet}$ with respect to $p_{T_{min}}^{ME}$ is needed; for the $Z/\gamma^* + jets$ production **AlpGen** authors recommend to choose the jet finder minimum p_T to be 5 GeV higher than the ME minimum p_T .

3 Generator configuration and analysis

Plots shown in this paper were obtained with an analysis coded in the Rivet [12, 13] MC Validation/Tuning framework. Rivet comes with an interface library, called **AGILE**, which provides interface to many event generators. The user can run the event generator through the **AGILE** interface and analyse the **HepMC** event record exploiting Rivet analysis classes. While Rivet can be used as an analysis framework for general studies on Monte Carlo event generators, as we did in this paper, its main feature is that it comes as a very straightforward tool to make comparisons to data.

In order to gain a more detailed understanding of the hard event simulation all the generators used in this work were run switching off the underlying event simulation. The analysis has been carried out at parton level. Also, the emission of final state photons from the leptons from the Z boson decay has been switched off. In the analysis, the lepton pair from the Z boson decay was required to have an invariant mass between 66 and 116 GeV.

4 Matrix element corrections in PYTHIA and HERWIG

4.1 Z boson transverse momentum

The p_T distribution for the lepton pair for inclusive Z/γ^* production in **PYTHIA** is shown in Fig. 6. Only the electron decay channel has been selected.

The three curves correspond to three different configurations: one is with ME corrections activated, the other two are obtained without matrix element correc-

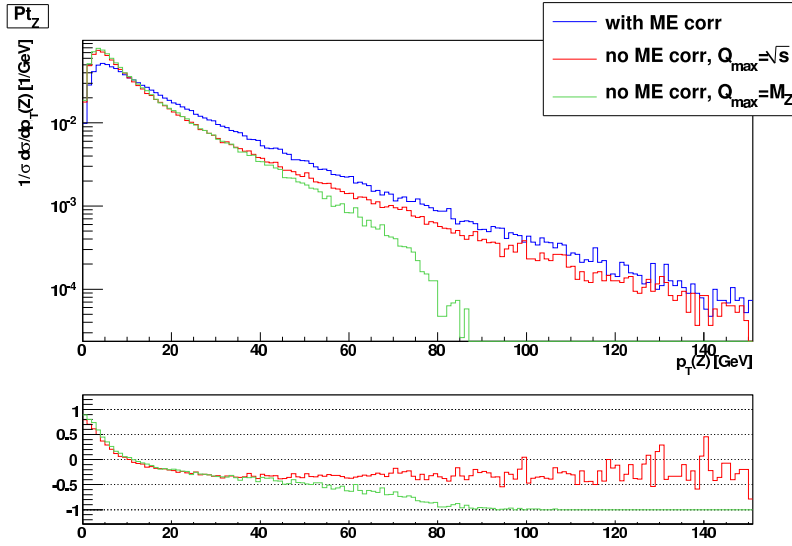


Figure 6: p_T spectrum for the lepton pair in PYTHIA for three different settings of the ISR: with ME corrections, without ME corrections and with the starting scale of the shower set to \sqrt{s} , without ME corrections and with the starting scale of the shower set to M_Z . The relative difference with respect to the curve with ME corrections is shown in the lower plot.

tions, but with different starting scales for the shower: the total hadronic center of mass energy and the invariant mass of the lepton pair respectively.

PYTHIA implements a virtuality ordered parton shower. The starting scale of the shower marks the maximum allowed virtuality in the shower evolution. If the starting scale is set to M_Z the hardest parton transverse momentum cannot exceed M_Z , thus also the Z p_T cannot exceed 90 GeV approximately, as shown in Fig. 6. When the starting scale is raised, the spectrum gets harder. When ME corrections are activated the spectrum gets even harder. The reason why the ME corrected spectrum is harder than the uncorrected one can be explained considering the relative amount of the two corrections at the LHC. The graph $gq \rightarrow Z/\gamma^*q$ contributes more than $q\bar{q} \rightarrow Z/\gamma^*g$, because \bar{q} is not a valence quark at LHC. We recall that Eq. (4) states that $W_{gq \rightarrow Z/\gamma^*q} > 1$, meaning that the first emission from the ME-corrected shower is done with a splitting probability higher than that of the uncorrected shower. Since the PS emission is always ordered, a higher splitting probability means that the probability for emitting a harder parton is higher than that of uncorrected shower. This explains why the corrected spectrum is harder than the uncorrected one. We also notice in passing that at the Tevatron $p\bar{p}$ collider [14, 15, 16] exactly the opposite holds: in that case $q\bar{q} \rightarrow Z/\gamma^*g$ dominates because \bar{q} is a valence quark; since the correction is < 1 for this graph (Eq. (3)) the ME corrected result is softer than the uncorrected one, as shown in [6].

One might expect that ME corrections should change the shape of spectra only at high p_T ; low p_T region should be well described by the parton shower alone.

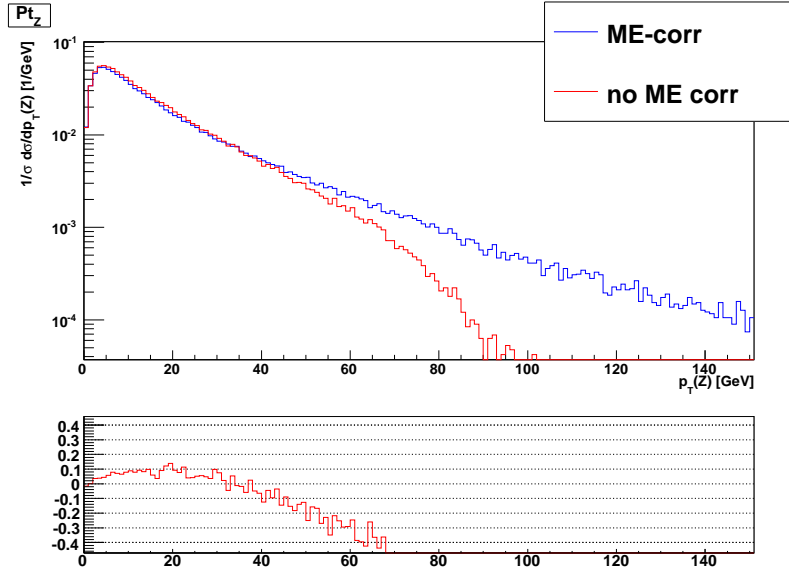


Figure 7: ME corrections effect in HERWIG in the Z p_T distribution. The effect at low p_T is small, while in PYTHIA the shape was different at low p_T as well.

Actually the Z p_T spectrum is altered by ME corrections all over the p_T range, as shown in Fig. 6. The three distributions are normalized, but the difference at low p_T is not only due to normalization; a change in shape is also present; such a change is testified by the relative difference plot, that does not flatten as p_T approaches zero. The reason for the change in shape at low p_T is that ME corrections change the Sudakov form factor used in the shower [17].

The Z p_T spectrum as obtained in HERWIG is shown in Fig. 7. Both the ME-corrected and the uncorrected spectra are shown. While ME corrections in PYTHIA change the whole shape of the distribution, also at low p_T , the change in shape at low p_T in HERWIG is small.

A comparison between ME corrected Z p_T distribution in PYTHIA and HERWIG is shown in Fig. 8. The agreement is very good all over the p_T spectrum.

4.2 Differential jet rates

To test how the phase space available for QCD radiation is filled we looked at differential jet rates. The differential jet rate $n \rightarrow n - 1$ is the distribution of the $n \rightarrow n - 1$ transition value, $Q_{n \rightarrow n-1}$, which is the value of the resolution parameter d_{cut} (in an exclusive k_\perp algorithm [18]) for which an n jet event turns into an $n - 1$ jet event. To understand what a differential jet rate is let's consider a simple example with three particles in the final state. Let the particles be 1, 2, 3. Let $d_{i,B}$ be the k_\perp distance of particle i from the beam line and $d_{i,j}$ be the k_\perp distance between particles i and j . Suppose that the sequence of ordered distances looks like this:

$$d_{1,B} < d_{2,B} < d_{1,2} < d_{3,B} < d_{1,3} < d_{2,3}. \quad (5)$$

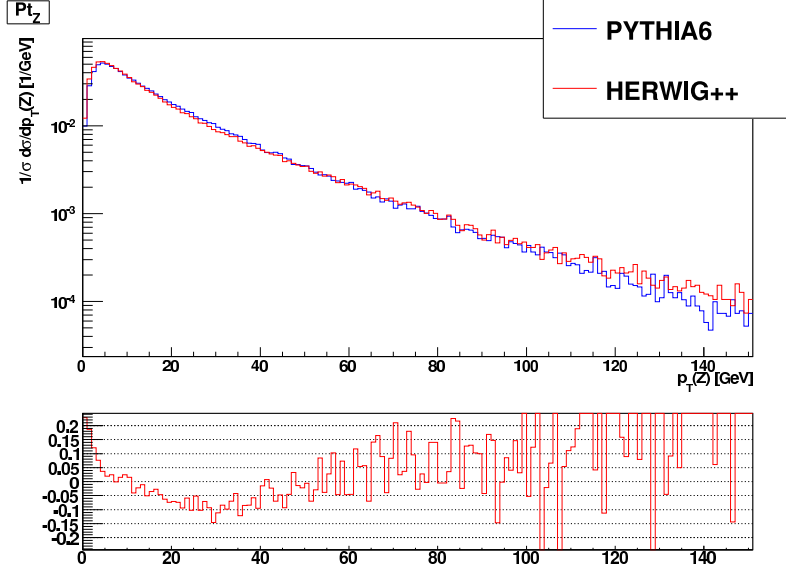


Figure 8: ME corrected Z p_T distribution in PYTHIA and HERWIG.

In an exclusive calculation the first jet that would be recombined with the beam line is particle 1, thus the $3 \rightarrow 2$ transition value is $Q_{3 \rightarrow 2} = d_{1,B}$. Then particle 2 is the next one to be recombined with the beam, thus $Q_{2 \rightarrow 1} = d_{2,B}$. At this point, if the d_{cut} is raised to be at least $d_{2,B}$ only $d_{3,B}$ survives in Eq. (5), thus $Q_{1 \rightarrow 0} = d_{3,B}$.

Let's now consider another example sequence:

$$d_{1,B} < d_{1,3} < d_{1,2} < d_{2,3} < d_{2,B} < d_{3,B}. \quad (6)$$

As before, $Q_{3 \rightarrow 2} = d_{1,B}$. If we raise d_{cut} to at least $d_{1,B}$ particle 1 gets clustered with the beam and the new sequence looks like

$$d_{2,3} < d_{2,B} < d_{3,B}, \quad (7)$$

so particles 2 and 3 are going to be clustered in the next step. Thus if d_{cut} is set to be at least equal to $d_{2,3}$ particles 2 and 3 are clustered, thus passing from 2 to 1 jet. Thus $Q_{2 \rightarrow 1} = d_{2,3}$. After they are clustered the sequence will have one only element, namely $d_{(2,3),B}$; thus $Q_{1 \rightarrow 0} = d_{(2,3),B}$.

Let's now see how the differential jet rates in PYTHIA look for the three setting of ME corrections. The $1 \rightarrow 0$ differential jet rate is shown in Fig. 9. The main differences among the three settings are in the region for high values of $Q_{1 \rightarrow 0}$. We see that the sample without ME corrections and with low starting shower scale is the one that dies first. This means that it is unable to fill the phase space for hard parton emission, which is responsible for filling the rightmost part of the plot. Regarding the other two settings we observe that they are similar, but while the sample without ME corrections tends to fill the region below 1, the one with ME corrections fills the region above 1 more, thus allowing for more radiation to be emitted.

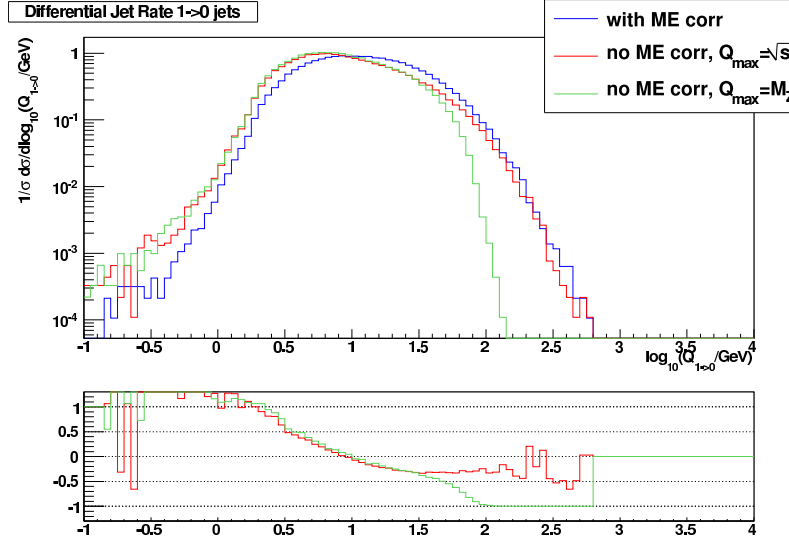


Figure 9: Distribution for the $1 \rightarrow 0$ differential jet rate in PYTHIA.

5 SHERPA and AlpGen compared to PYTHIA

As mentioned in the introduction, we made a consistency check of the matching prescriptions implemented in SHERPA and AlpGen. The test consists in the comparisons of the observables obtained with ME corrected PYTHIA with those obtained with AlpGen and SHERPA when at most one additional parton is allowed to come from the ME calculation. This approach has been already explored in [19] to test various matching prescriptions in e^+e^- collisions.

5.1 SHERPA

The total cross section for inclusive Z/γ^* is calculated in PYTHIA at Leading Order accuracy, i.e. it is calculated from the process $q\bar{q} \rightarrow e^+e^-$; the subsequent PS, either corrected or uncorrected, happens with probability 1, so it cannot modify the cross section. In SHERPA the cross section comes as a sum over the different selected final state parton multiplicities.

$$\sigma_{\text{SHERPA}} = \sum_{i=0}^N \sigma_i \langle w_i \rangle \quad (8)$$

where σ_i is the cross section for i additional partons in the final state and $\langle w_i \rangle$ is the average Sudakov weight for that configuration.

Table 1 shows the cross section values as obtained in PYTHIA and in SHERPA for four different values of the resolution cut q_{cut} that steers the separation between the ME and the PS regions.

The difference in the total cross section with respect to PYTHIA is up to about 10%, for the sample with the lowest value of q_{cut} . Cross sections for both SHERPA and

SHERPA		σ_i [pb]	$\langle w_i \rangle$	Total σ [pb]
$q_{cut}=10\text{GeV}$	0 jet	838.9	0.7489	1383
	1 jet	998.7	0.7559	
$q_{cut}=20\text{GeV}$	0 jet	1059.5	0.9301	1405
	1 jet	484.6	0.8657	
$q_{cut}=40\text{GeV}$	0 jet	1271.2	0.9992	1434
	1 jet	177.2	0.9267	
$q_{cut}=500\text{GeV}$	0 jet	1926.6	0.7540	1453
	1 jet	0.038	0.9802	
PYTHIA				Total σ [pb]
inclusive				1528

Table 1: Cross sections for SHERPA and PYTHIA.

PYTHIA are formally LO; some differences are due to the q_{cut} dependency mainly. If one takes a very high value for q_{cut} , this makes SHERPA get closer and closer to PYTHIA. In fact, as q_{cut} is increased the contribution to the total cross section from the configuration with one additional parton vanishes, thus leaving the leading order contribution alone, which is the only one considered in PYTHIA for the cross section calculation. In summary the dependency on q_{cut} in SHERPA is of the order of 5-10%. Even when higher order emissions are completely removed there is a 5% discrepancy with PYTHIA. This presumably happens due to differences in the choice of scales in the two generators. In particular in SHERPA the renormalization scale is set to the q_{cut} value.

The p_T spectrum for the lepton pair in SHERPA and PYTHIA is shown in Fig. 10 (a). As mentioned above, SHERPA has been run such that only one additional parton can be emitted from the matrix element.

SHERPA has been run with three different values of the parameter q_{cut} that governs the separation between the phase space region filled by the ME and the region filled by the PS. The values used were $q_{cut}=10, 20, 40$ GeV. As described in Sec. 2.2 the region above q_{cut} is filled by a modified ME, in which Sudakov form factors are attached to the ME, while the region below the cut is filled by a vetoed PS. SHERPA appears to closely follow the PYTHIA spectrum. Some discrepancies are observed in the first few bins. These are most probably due to a different tuning for the primordial p_T^2 distribution of partons in the protons. We notice in particular that the high p_T tail, that is sensitive to additional hard emission, appears to be correctly reproduced. We also observe a small dependence on the value of q_{cut} : the three curves for SHERPA agree within few percent.

The pseudorapidity η distribution for the lepton pair is shown in Fig. 10 (b). The distributions from SHERPA well agree with PYTHIA in the central region, where

²The primordial p_T distribution of partons in protons, often referred to as primordial k_\perp is the transverse momentum distribution of partons in the hadrons entering the collision. The primordial k_\perp models a soft non-perturbative effect.

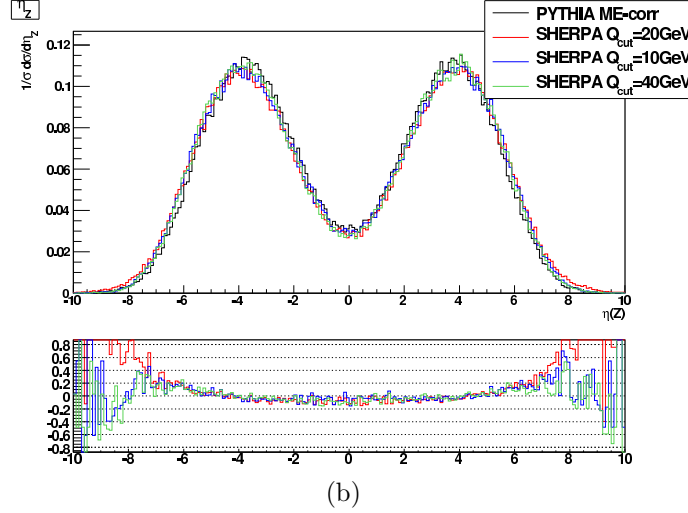
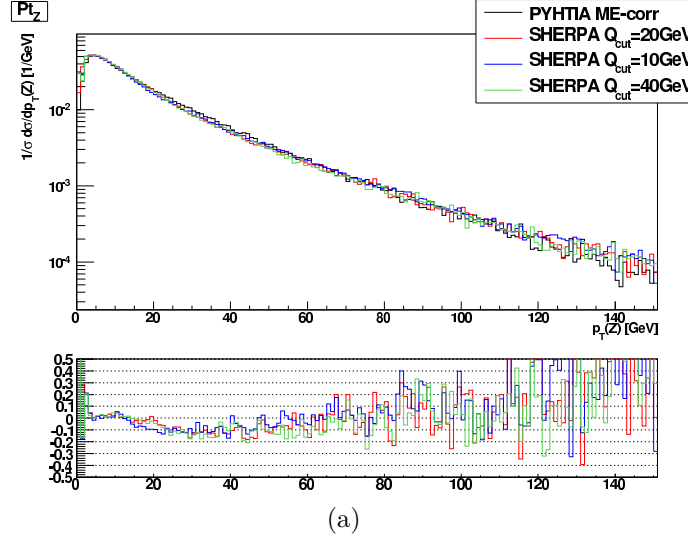


Figure 10: p_T spectrum (a) and η distribution (b) for the lepton pair in PYTHIA and SHERPA. The latter has been run with at most one additional parton from the ME; three different values for the separation cut between ME and PS regions have been used: $q_{cut} = 10, 20, 40$ GeV.

the difference is within 10-15%; in the tails of the distribution difference is more evident.

The p_T distribution for the positive lepton is shown in Fig. 11. In this case too SHERPA agrees with PYTHIA, without strong dependency on the resolution cut q_{cut} .

Concerning the QCD observables we looked at differential jet rates. The distribution for the rate $1 \rightarrow 0$ in PYTHIA and in SHERPA is shown in Fig. 12. For SHERPA we tried three different values for the matching parameter q_{cut} : 10, 20, 40 GeV. The vertical lines shown in the plots indicate the position of the resolution parameter q_{cut} . In SHERPA, the phase space above q_{cut} is filled by the Matrix Element, while

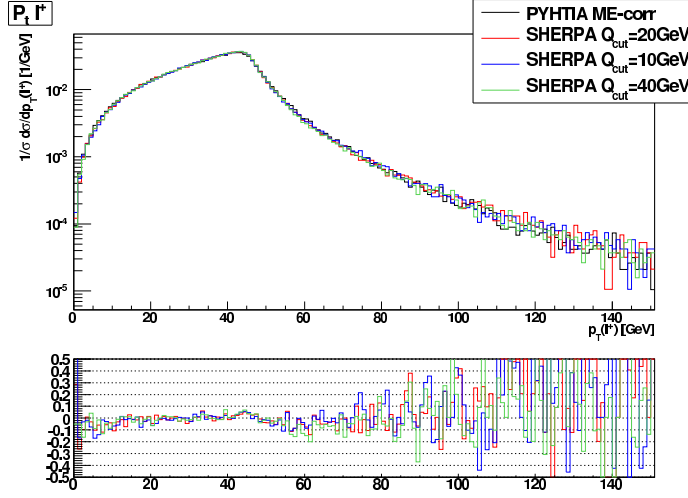


Figure 11: p_T distributions for the positive lepton.

the region below q_{cut} is filled by the vetoed shower.

SHERPA agrees well with PYTHIA. The transition between the ME- and PS-populated regions is quite smooth for all the three values used for q_{cut} . The relative difference with respect to PYTHIA is at most 20%, in the vicinities of the q_{cut} region. The tail for very low values of $Q_{1\rightarrow 0}$ shows some differences, that can be due to slightly different settings for the primordial k_\perp .

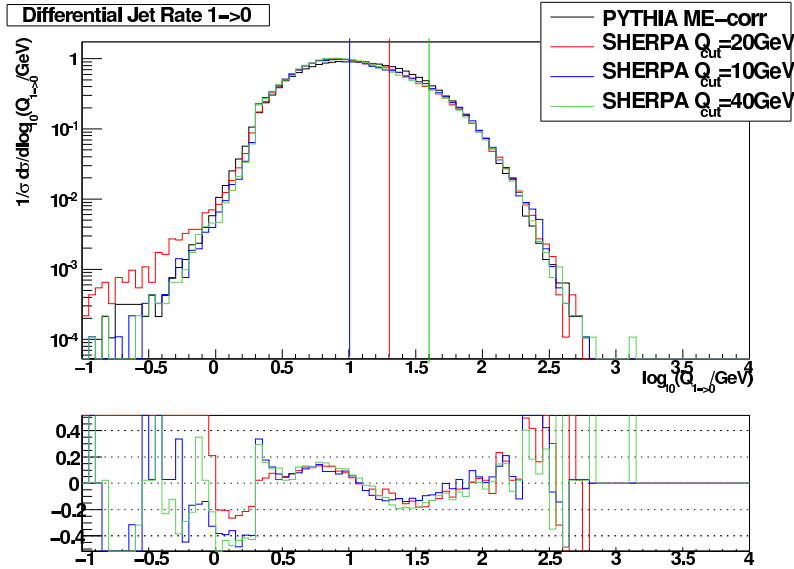


Figure 12: Differential jet rate $1 \rightarrow 0$ in PYTHIA and SHERPA. For SHERPA we used three values for the matching parameter q_{cut} : 10, 20, 40 GeV. Relative differences are calculated with respect to PYTHIA.

5.2 AlpGen plus PYTHIA

We made the same test with **AlpGen**, looking for differences with respect to ME corrected **PYTHIA**. We considered the contribution from up to one additional parton from the matrix element, and we used **PYTHIA** to shower the ME events generated by **AlpGen**.

AlpGen		σ_i [pb]	Total σ [pb]
ME cutoff=10GeV	0 jet	1092	1609
	1 jet	517	
ME cutoff=20GeV	0 jet	1303	1594
	1 jet	291	
ME cutoff=40GeV	0 jet	1452	1558
	1 jet	106	
PYTHIA			Total σ [pb]
inclusive			1528

Table 2: Cross sections for **AlpGen** and **PYTHIA**.

Table 2 summarizes the total cross section for **AlpGen** with up to one additional parton from the ME. Results for three values of the ME cutoff for the generation of the additional jet are shown. The difference with respect to **PYTHIA** is 5% at most.

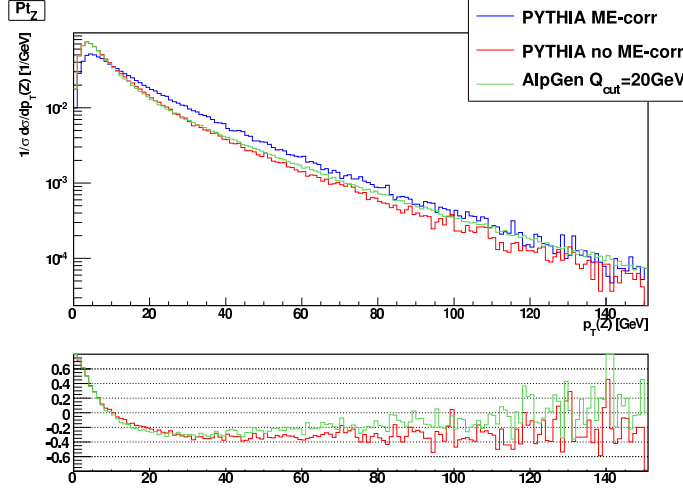
The p_T spectrum and the η distribution for **PYTHIA** (with and without ME corrections) and **AlpGen** are shown in Fig. 13. Concerning **PYTHIA**, the sample without ME corrections has the shower starting scale set to \sqrt{s} . For **AlpGen** we used a minimum p_T for the additional ME generated parton of 20 GeV, and the minimum p_T for the cone algorithm that steers the matching was set to 25 GeV, as recommended by the authors.

AlpGen lepton pair p_T spectrum appears to be softer than ME-corrected **PYTHIA**. This also translates into a broader η distribution for **AlpGen**. If we compare **AlpGen** to both ME corrected and to uncorrected **PYTHIA**, it appears that **AlpGen** follows uncorrected **PYTHIA** for low p_T values and then agrees with corrected **PYTHIA** in the high p_T tail.

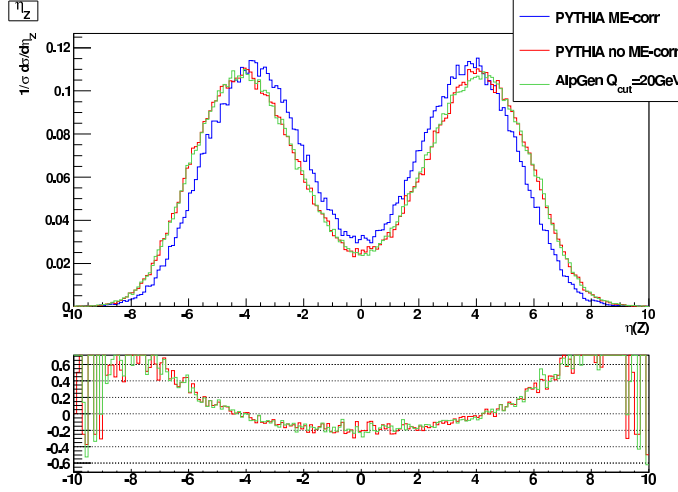
We think that this effect is not related to **AlpGen** itself but rather to **PYTHIA**. When **PYTHIA** is used to shower **AlpGen** events **PYTHIA**'s native ME corrections are switched off, because **AlpGen** is going to supply such corrections. As noticed in Fig. 6, the side effect of switching off ME corrections in **PYTHIA** is that the low p_T shape changes. **AlpGen** cannot modify the low p_T region, which is completely determined by the PS; it can only add high p_T radiation which is actually what it does.

Also the p_T spectrum for the leptons from the Z boson decay (Fig. 14) shows the same behavior.

The dependency on the resolution cut that separates the ME from the PS region is very limited. The lepton pair p_T and η spectra and the p_T spectrum for



(a)



(b)

Figure 13: p_T spectrum (a) and η distribution (b) for the lepton pair. **AlpGen** is compared with **PYTHIA**, with and without ME corrections. Relative difference with respect to ME corrected **PYTHIA** is shown for each plot.

the electron from Z are shown in Fig. 15 for three different choices of the Matrix Element cutoff in **AlpGen** (and correspondingly of the minimum p_T of the internal cone algorithm): $q_{cut}=10, 20, 40$ GeV.

Concerning QCD observables, differential jet rate plots appear to confirm the trend observed for leptonic observables. Fig. 16 shows the $1 \rightarrow 0$ differential jet rate. Both ME corrected and uncorrected **PYTHIA** are shown as a reference. We see that **AlpGen** closely follows uncorrected **PYTHIA** in the low $Q_{1 \rightarrow 0}$ region, then it starts to agree with corrected **PYTHIA** for high values of $Q_{1 \rightarrow 0}$.

Fig. 17 shows the $1 \rightarrow 0$ differential jet rate in **AlpGen** for three different values of the ME cutoff in **AlpGen**. Also ME-corrected **PYTHIA** is shown as a reference.

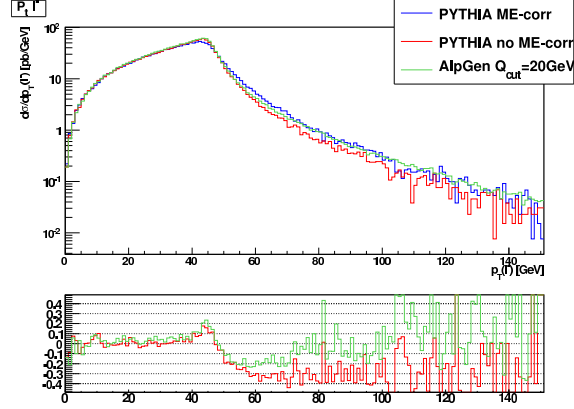


Figure 14: p_T spectrum of the electron from Z decay. AlpGen is compared with PYTHIA, with and without ME corrections. Relative differences are with respect to ME-corrected PYTHIA.

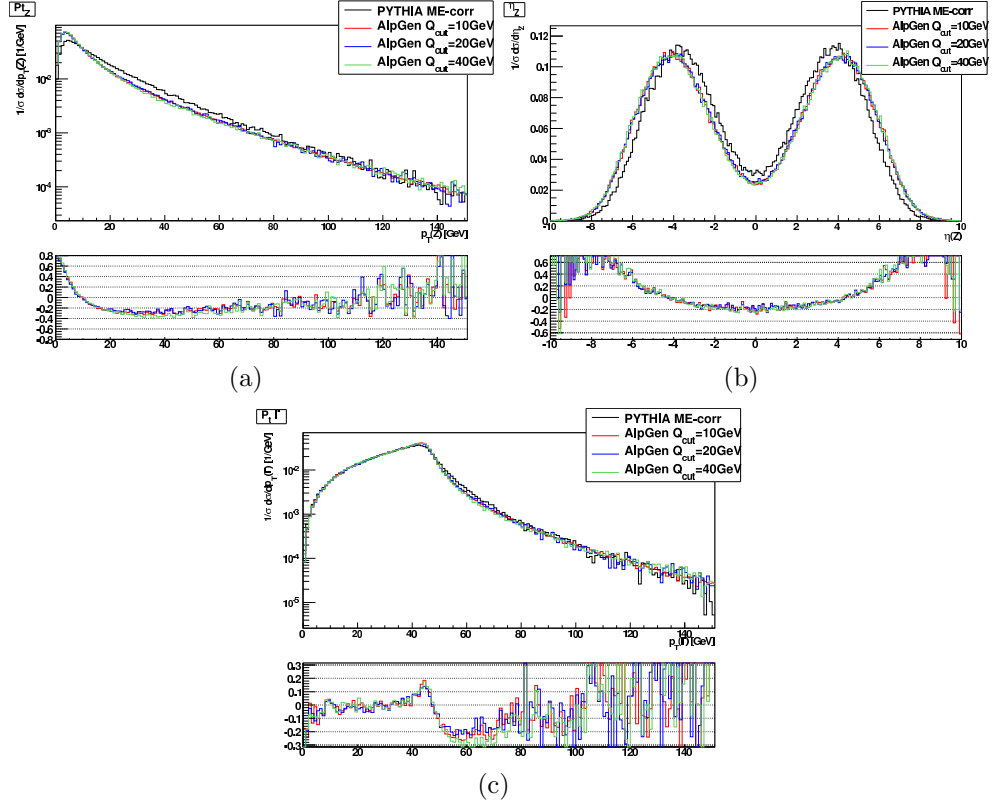


Figure 15: (a) p_T spectrum and (b) η distribution for the lepton pair. (c) p_T spectrum for the electron. AlpGen has been run with three different values of the Matrix Element cutoff. Also ME-corrected PYTHIA is shown as a reference. Relative differences are calculated with respect to ME-corrected PYTHIA.

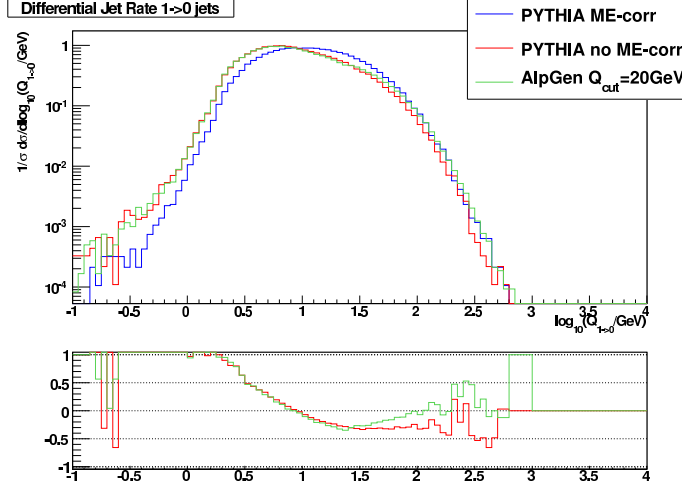


Figure 16: Differential jet rate for the $1 \rightarrow 0$ transition. **AlpGen** has been run with a ME cutoff of 20 GeV. Both ME corrected and uncorrected (starting shower scale set to \sqrt{s}) **PYTHIA** are shown as a reference. Relative differences are with respect to ME corrected **PYTHIA**.

The dependency on the cut is very limited, as already observed for the leptonic observables.

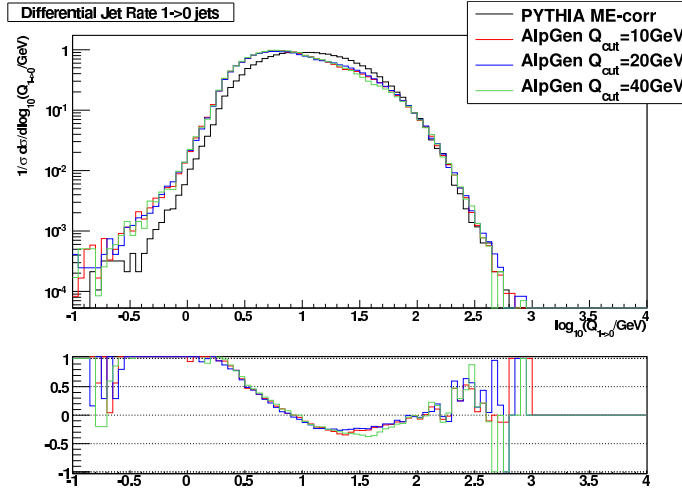


Figure 17: Differential jet rates for the transitions $1 \rightarrow 0$. **AlpGen** has been run with three different values of the Matrix Element cutoff. Also ME-corrected **PYTHIA** is shown as a reference. Relative differences are with respect to ME corrected **PYTHIA**.

5.3 **AlpGen** plus **HERWIG**

We tried to shower **AlpGen** events also with **HERWIG**. We observed that using **HERWIG** gives results much more consistent with the **PYTHIA** benchmark. The Z boson trans-

verse momentum as obtained in **AlpGen**+**HERWIG** is shown in Fig. 18. ME corrected **PYTHIA** spectrum is reported in the same plot as a reference. The agreement is much better than it was using **PYTHIA** as a parton shower (Fig. 13 (a)). The low p_T region, that was not reproduced in **AlpGen**+**PYTHIA** is now well reproduced within few percent, except for the very first bins that may be affected by different primordial k_\perp tunings.

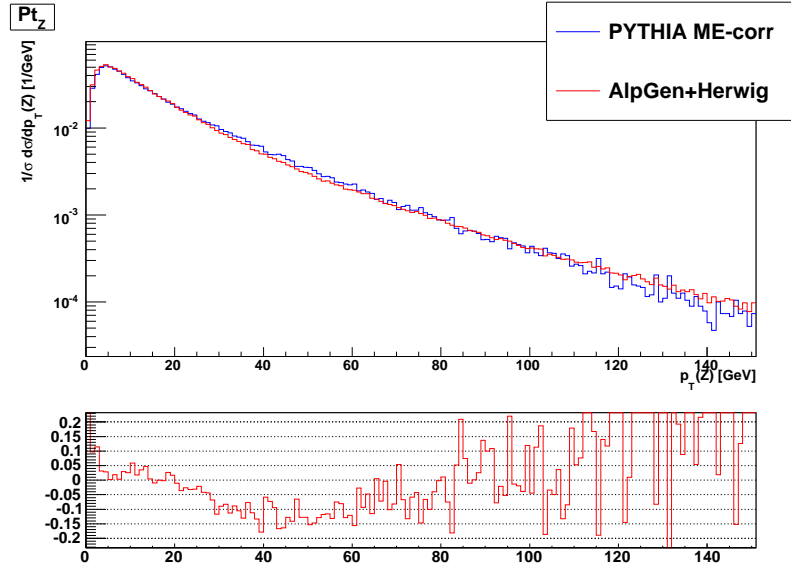


Figure 18: Z boson transverse momentum as obtained in **AlpGen**+**HERWIG** and in **PYTHIA**.

6 Conclusion

We studied the effect of ME corrections in **PYTHIA** and **HERWIG**. Both programs can fully take into account ME corrections for one additional parton emission. The implementation is slightly different.

- **PYTHIA** modifies the shower in two steps: first the starting scale is raised so that any hard emission from the shower is kinematically possible; then the emission probability for the first emission is modified to include ME correction effect.
- In **HERWIG** the shower leaves the phase space for hard emission completely uncovered. For this reason the correction is performed in two steps: in the region already filled by the shower the same approach as **PYTHIA** is used. In the remaining part of the phase space the ME for one additional parton emission is directly used.

Both approaches give similar results. When ME corrections are switched off the Z p_T spectrum in PYTHIA changes also at low p_T , while the low p_T shape in HERWIG remains unchanged.

We used ME corrected PYTHIA as a test bed for SHERPA and AlpGen. When those programs are allowed to emit at most one parton from the ME calculation they should give results similar to PYTHIA. Actually SHERPA follows PYTHIA quite well, both on lepton and jet observables. On the other hand AlpGen+PYTHIA appears to follow uncorrected PYTHIA at low p_T , for example it shows softer Z p_T spectrum with respect to ME corrected PYTHIA. This can be traced down to the fact that when PYTHIA is used to shower events produced by AlpGen ME corrections are switched off. This is done because AlpGen is going to introduce its own corrections. The side effect of this is that the low p_T shape of the Z p_T spectrum changes, and AlpGen cannot do anything in that region, which is entirely determined by the PS alone. AlpGen can only modify the high p_T tail of the distribution.

Using HERWIG to shower AlpGen events turns out to be in much better agreement with the PYTHIA benchmark. When using HERWIG to shower AlpGen events native HERWIG ME corrections are switched off (like in PYTHIA) but this does not affect the low p_T shape, which remains correct.

The dependency on the cut used to separate the ME and PS regions is limited both in AlpGen and in SHERPA.

Acknowledgements

We would like to thank Prof. F. Krauss, Dr. F. Piccinini, Prof. S. Catani for many useful discussions.

This work was supported by the Marie Curie Research Training Network “MC-net” (contract number MRTN-CT-2006-035606).

References

- [1] T. Sjostrand, S. Mrenna, and P. Skands, “PYTHIA 6.4 physics and manual,” *JHEP* **05** (2006) 026, [arXiv:hep-ph/0603175](#).
- [2] G. Corcella *et al.*, “HERWIG 6.5 release note,” [arXiv:hep-ph/0210213](#).
- [3] M. Bahr *et al.*, “Herwig++ Physics and Manual,” *Eur. Phys. J.* **C58** (2008) 639–707, [arXiv:0803.0883 \[hep-ph\]](#).
- [4] M. L. Mangano, M. Moretti, F. Piccinini, R. Pittau, and A. D. Polosa, “ALPGEN, a generator for hard multiparton processes in hadronic collisions,” *JHEP* **07** (2003) 001, [arXiv:hep-ph/0206293](#).
- [5] T. Gleisberg *et al.*, “Event generation with SHERPA 1.1,” *JHEP* **02** (2009) 007, [arXiv:0811.4622 \[hep-ph\]](#).

- [6] G. Miu and T. Sjostrand, “W production in an improved parton shower approach,” *Phys. Lett.* **B449** (1999) 313–320, [arXiv:hep-ph/9812455](#).
- [7] M. H. Seymour, “Matrix element corrections to parton shower algorithms,” *Comp. Phys. Commun.* **90** (1995) 95–101, [arXiv:hep-ph/9410414](#).
- [8] G. Corcella and M. H. Seymour, “Initial state radiation in simulations of vector boson production at hadron colliders,” *Nucl. Phys.* **B565** (2000) 227–244, [arXiv:hep-ph/9908388](#).
- [9] S. Catani, F. Krauss, R. Kuhn, and B. R. Webber, “QCD matrix elements + parton showers,” *JHEP* **11** (2001) 063, [arXiv:hep-ph/0109231](#).
- [10] F. Krauss, “Matrix elements and parton showers in hadronic interactions,” *JHEP* **08** (2002) 015, [arXiv:hep-ph/0205283](#).
- [11] M. Mangano, “The so-called MLM prescription for ME/PS matching,” October, 4, 2002. Talk presented at the Fermilab ME/MC Tuning Workshop.
- [12] “Rivet web page,” 2008. <http://projects.hepforge.org/rivet/>.
- [13] A. Buckley *et al.*, “CEDAR: Progress and status report,” *J. Phys. Conf. Ser.* **119** (2008) 052006.
- [14] “Design report Tevatron 1 project,”. FERMILAB-DESIGN-1983-01.
- [15] **CDF IIb** Collaboration, P. T. Lukens, “The CDF IIb detector: Technical design report,”. FERMILAB-TM-2198.
- [16] **D0** Collaboration, V. M. Abazov *et al.*, “Run IIb upgrade technical design report,”. FERMILAB-PUB-02-327-E.
- [17] T. Sjostrand and S. Mrenna. Private communication.
- [18] S. Catani, Y. L. Dokshitzer, M. H. Seymour, and B. R. Webber, “Longitudinally invariant K(t) clustering algorithms for hadron hadron collisions,” *Nucl. Phys.* **B406** (1993) 187–224.
- [19] N. Lavesson and L. Lonnblad, “Merging parton showers and matrix elements – back to basics,” *JHEP* **04** (2008) 085, [arXiv:0712.2966 \[hep-ph\]](#).